

Chemical Yields from Hypernovae and Abundance Profiling of Extremely Metal-Poor Stars

Ken'ichi Nomoto*

Kavli Institute for the Physics and Mathematics of the Universe, The University of Tokyo

E-mail: nomoto@astron.s.u-tokyo.ac.jp

Tomoharu Suzuki

College of Engineering, Chubu University

E-mail: tsuzuki@isc.chubu.ac.jp

We examine how the chemical yields of Hypernovae (HNe) and Faint supernovae (SNe) are related to some peculiar abundance patterns observed in extremely metal-poor (EMP) stars. Such studies provide useful constraints on the explosion mechanisms and the nature of first stars. Nucleosynthesis in Hypernovae is characterized by larger abundance ratios (Zn,Co,V,Ti)/Fe than normal SNe, which can explain the observed ratios in EMP stars. Nucleosynthesis in Faint SNe is characterized by a large amount of fall-back, which explains the abundance pattern of carbon-enhanced EMP (CEMP) stars. The abundance patterns of ultra metal-poor (UMP) and hyper metal-poor (HMP) stars can also be explained with chemical yields from these types of explosions. These comparisons suggest that black-hole-forming SNe made important contributions to the early Galactic (and cosmic) chemical evolution.

XII International Symposium on Nuclei in the Cosmos,

August 5-12, 2012

Cairns, Australia

*Speaker.

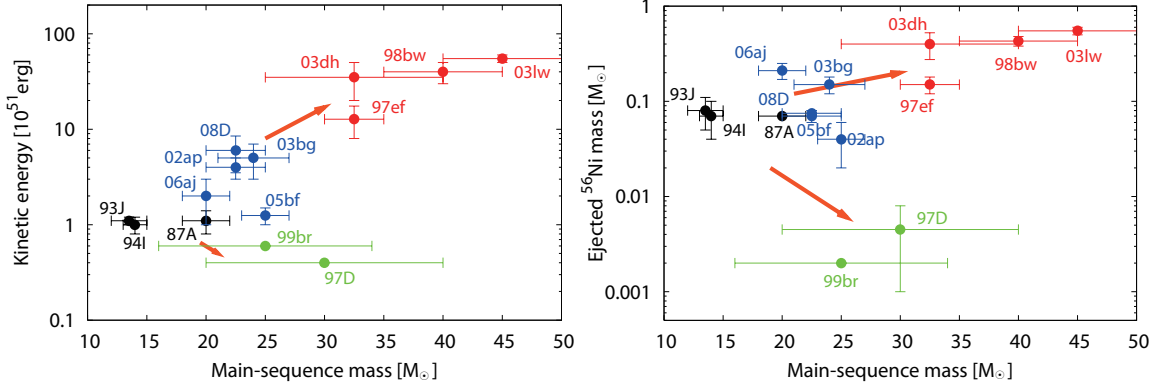


Figure 1: The explosion energy and the ejected ^{56}Ni mass as a function of the main-sequence mass of the progenitors for several supernovae/hypernovae.

1. Introduction: Hypernovae and Faint Supernovae

In the early universe with extremely small metal content, the enrichment by a single supernova (SN) can dominate the preexisting metal contents. Then the abundance pattern of the enriched gas may reflect nucleosynthesis in the individual SN. The second generation stars are formed from the enriched gas and the long-lived low mass stars may be observed as extremely metal-poor (EMP) and hyper metal-poor (HMP) stars [2]. Thus the abundance patterns of EMP/HMP stars can constrain the nucleosynthetic yields of the Pop III SN and thus the mass range of first stars.

Actually, recent observations discovered several EMP/HMP stars, whose abundance patterns are quite unusual (e.g., [2]), being significantly different from previously known nucleosynthesis yields of massive stars. These new observations of EMP/HMP stars make important challenges to the stellar evolution/nucleosynthesis theory.

Interestingly, there is another challenge to the conventional stellar evolution and supernova models. That is the establishment of the Gamma-Ray Burst (GRB)-Supernova Connection (e.g., [35]). Four GRB-associated SNe have been confirmed spectroscopically so far. They are all very energetic supernovae, whose kinetic energy E exceeds 10^{52} erg, more than 10 times the kinetic energy of normal core-collapse SNe. (We use the explosion energy E for the final kinetic energy of explosion.)

We can estimate M , E , and the mass of ^{56}Ni as shown in Figure 1 [19, 21] from the comparison between the observed and calculated spectra and light curves of supernovae. In the present paper, we use the term 'Hypernova (HN)' to describe such a hyper-energetic supernova with $E_{51} = E/10^{51}$ erg $\gtrsim 10$.

SNe from $M \gtrsim 25M_{\odot}$ form BHs and seem to bifurcate into the Hypernova branch and the Faint SNe branch. If the BH has little angular momentum, little mass ejection would take place and be observed as Faint SNe. On the other hand, a rotating BH could eject a matter in a form of jets to make a Hypernova. The latter explosions produce a large amount of heavy elements from α -elements and Fe-peak elements.

Nucleosynthesis features in such hyper-energetic supernovae must show some important differences from normal supernova explosions. This might be related to the unpredicted abundance

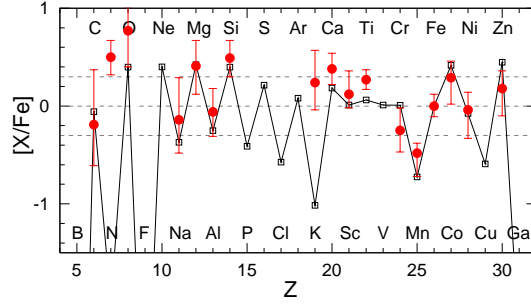


Figure 2: Comparison between the abundance pattern of VMP stars at $-2.7 < [\text{Fe}/\text{H}] < -2.0$ [5, filled circles with error bars] and the IMF integrated yield of Pop III SNe from $10M_{\odot}$ to $50M_{\odot}$ [26]. The horizontal dashed lines indicate the conventional theoretical error bars of a factor of 2.

patterns observed in the extremely metal-poor (EMP) halo stars. This approach leads to identifying the First Stars in the Universe, i.e., metal-free, Population III (Pop III) stars which were born in a primordial hydrogen-helium gas cloud. This is one of the important challenges of the current astronomy.

2. Abundance Profiling of Extremely Metal-Poor Stars

In the following sections, we present our attempt to compare the SN yields and the abundance patterns of EMP stars. EMP stars are classified into three groups according to $[\text{C}/\text{Fe}]$:

- (1) $[\text{C}/\text{Fe}] \sim 0$, normal EMP stars ($-4 < [\text{Fe}/\text{H}] < -3$) [5];
- (2) $[\text{C}/\text{Fe}] \gtrsim +1$, Carbon-enhanced EMP (CEMP) stars ($-4 < [\text{Fe}/\text{H}] < -3$, e.g., CS 22949–37) [10];
- (3) Ultra metal-poor (UMP) stars ($-5 < [\text{Fe}/\text{H}] < -4$) with carbon-enhancement (e.g., HE 0557-4840 [22]) or without C-enhancement (e.g., SDSS J102915+172927 [4]).
- (4) $[\text{C}/\text{Fe}] \sim +4$, hyper metal-poor (HMP) stars ($[\text{Fe}/\text{H}] < -5$, e.g., HE 0107–5240 [6, 3]; HE 1327–2326 [11]).

2.1 Very Metal-Poor (VMP) Stars

VMP stars defined as $[\text{Fe}/\text{H}] \lesssim -2.5$ [2] are likely to have the abundance pattern of well-mixed ejecta of many SNe. In Figure 2, we thus compare the abundance patterns of VMP stars with the SN yields integrated over the progenitors of 10 - $50M_{\odot}$ [26], which shows that many elements are in reasonable agreements.

However, N is underproduced in these models. There are two possible explanations for this discrepancy: (1) N was underproduced in the Pop III SN as in these models, but was enhanced as observed during the first dredge-up in the low-mass red-giant EMP stars [24, 34]. Actually, most EMP stars are red-giants. (2) N was enhanced in massive progenitor stars before the SN explosion. N is mainly synthesized by the mixing between the He convective shell and the H-rich envelope (e.g., [30, 14]). Mixing can be enhanced by rotation [13, 17]. Suppose that the Pop III SN progenitors were rotating faster than more metal-rich stars because of smaller mass loss, then $[\text{N}/\text{Fe}]$ was enhanced as observed in EMP stars.

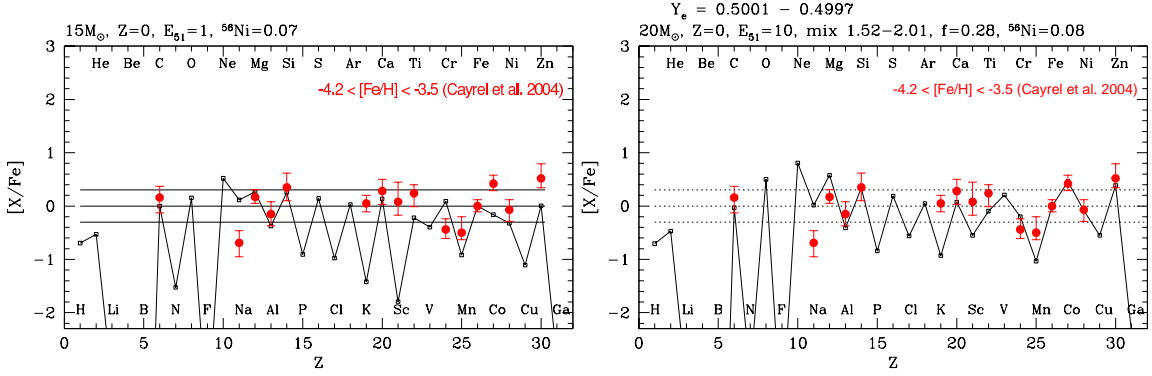


Figure 3: Averaged elemental abundances of stars with $-4.2 < [\text{Fe}/\text{H}] < -3.5$ [5, filled circles with error bars] compared with the normal SN yield (left: $15 M_{\odot}$, $E_{51} = 1$) and the HN yield (right: $20 M_{\odot}$, $E_{51} = 10$).

For underproduction of potassium, the neutrino absorption during the core-collapse may enhance Y_e and thus $[\text{K}/\text{Fe}]$ near the mass cut.

2.2 Extremely Metal-Poor (EMP) Stars

In the early galactic epoch when the galaxy was not yet chemically well-mixed, each EMP star may be formed mainly from the ejecta of a single Pop III SN (e.g., [29]). The formation of EMP stars was driven by a supernova shock, so that $[\text{Fe}/\text{H}]$ was determined by the ejected Fe mass and the amount of circumstellar hydrogen swept-up by the shock wave [23]. Then, hypernovae with larger E are likely to induce the formation of stars with smaller $[\text{Fe}/\text{H}]$, because the mass of interstellar hydrogen swept up by a hypernova is roughly proportional to E [23] and the ratio of the ejected iron mass to E is smaller for hypernovae than for normal supernovae.

Figure 3 shows that the averaged abundances of EMP stars ($-4.2 < [\text{Fe}/\text{H}] < -3.5$) can be fitted well with the hypernova model of $20 M_{\odot}$ and $E_{51} = 10$ (right) but not with the normal SN model of $15 M_{\odot}$ and $E_{51} = 1$ (left) [20, 26].

In the normal SN model (left), the yields are in reasonable agreements with the observations for the ratios $[(\text{Mg}, \text{Si}, \text{Ca})/\text{Fe}]$, but give too small $[(\text{Mn}, \text{Co}, \text{Zn})/\text{Fe}]$ and too large $[(\text{Na}, \text{Cr})/\text{Fe}]$.

In the HN model (right), $[(\text{Cr}, \text{Co}, \text{Zn})/\text{Fe}]$ are in much better agreement with observations, and $[(\text{K}, \text{Sc}, \text{Ti})/\text{Fe}]$ are improved. The ratios of Co/Fe and Zn/Fe are larger in higher energy explosions since both Co and Zn are synthesized in complete Si burning at high temperature region (see the next subsection). To account for the observations, materials synthesized in a deeper complete Si-burning region should be ejected, but the amount of Fe should be small. This is realized in the mixing-fallback models [31, 33].

2.3 Carbon-Enhanced Extremely Metal-Poor (CEMP) Stars

Stars with large $[\text{C}/\text{Fe}]$ (~ 1), called C-rich EMP (CEMP) stars, are discussed in [32, 33]. The origin of those stars may be different from those of $[\text{C}/\text{Fe}] \sim 0$ stars. The large $[\text{C}/\text{Fe}]$ ($\gtrsim 0.5$) can be understood as the faint SN origin, because the faint SNe are characterized by a large amount of Fe fallback that leads to large $[(\text{C}, \text{N}, \text{O})/\text{Fe}]$ [32, 33]. Figure 4 (left) shows the comparison between the abundance pattern of a C-rich EMP star (CS 29498-043: [1]) and the $25 M_{\odot}$ faint SN model [26].

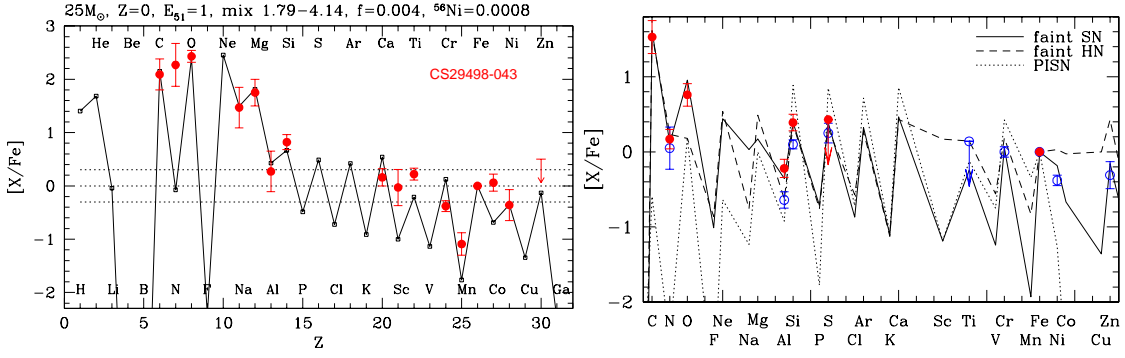


Figure 4: (left:) Comparison between the abundance pattern of the C-rich EMP (CEMP) star (CS 29498-043: *filled circles with error bars* [1]) and the theoretical yields of the $25 M_{\odot}$ faint SN (*solid line* [26]). (right:) The elemental abundance pattern of the metal-poor C-rich DLA (*filled circles*) and peculiar DLA (*open circles*) [8, 9]. The solid and short-dashed lines show the nucleosynthesis yields of faint core-collapse supernovae from $25 M_{\odot}$ stars with mixing-fallback. The dotted line is for pair-instability supernovae from $170 M_{\odot}$ stars [16].

Most C-rich EMP stars show O/Mg being significantly larger than the solar ratio. Faint SNe enhance [O/Fe] more effectively than [Mg/Fe], because Mg is synthesized in the inner region and thus fallen-back onto the central remnant more preferentially than O. (Note that the abundance determination of O is subject to the uncertain hydrodynamical (3D) effects [18].)

2.4 Ultra Metal-Poor (UMP) Stars

At $[\text{Fe}/\text{H}] = -4.75$, the ultra metal-poor (UMP) star HE0557-4840 shows a medium carbon enhancement of $[\text{C}/\text{Fe}] = +1.6$ [22], which is smaller than that of HMP stars.

It is interesting to note that the abundance pattern of the very metal-poor ($[\text{Fe}/\text{H}] \sim -3$) and C-enhanced ($[\text{C}/\text{Fe}] \sim +1.53$) DLA [9] is similar to those of EMP stars such as the ultra metal-poor star HE0557-4840. Figure 4 (right) shows that the abundance pattern of this DLA is better reproduced by the $25 M_{\odot}$ explosion model rather than a pair-instability SN [16]. Chemical enrichment by the first stars in the first galaxies is likely to be driven by core-collapse supernovae.

At $[\text{Fe}/\text{H}] = -4.89$, SDSS J102915+172927 [4] does not indicate a large enhancement of carbon, nitrogen and oxygen, and thus this stars has the lowest $Z \leq 7.40 \times 10^{-7}$ ever detected. The elemental abundance pattern is rather consistent with core-collapse supernovae reproducing the EMP stars (Fig.5: left).

2.5 Hyper Metal-Poor (HMP) Stars

Two HMP stars, HE0107-5240 [6] and HE1327-2326 [11], have metallicity of $[\text{Fe}/\text{H}] < -5$. These discoveries have raised an important question as to whether the observed low mass ($\sim 0.8 M_{\odot}$) HMP stars are actually Pop III stars, or whether these HMP stars are the second generation stars being formed from gases which were chemically enriched by a single Pop III SN [32]. This is related to the questions of how the initial mass function depends on the metallicity. Thus identifying the origin of these HMP stars is indispensable to the understanding of the earliest star formation and chemical enrichment history of the Universe.

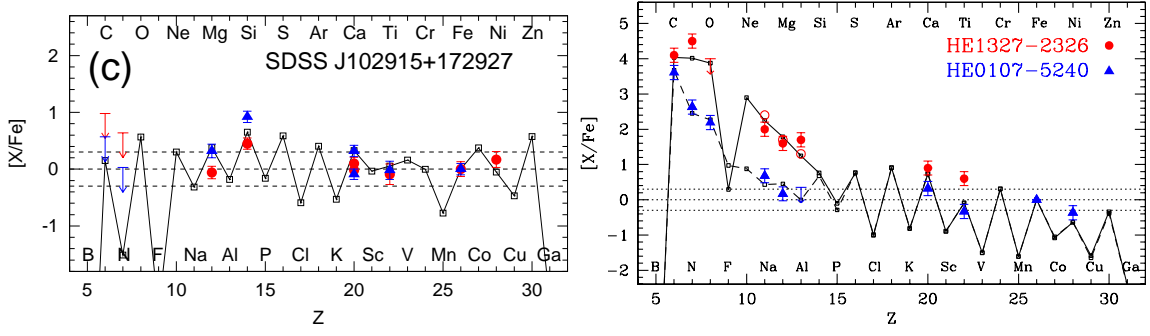


Figure 5: (left) Elemental abundances of the UMP star SDSS J102915+172927 [4] compared with the core-collapse SN yield [28]. (right) C-rich HMP stars HE0107-5240 (filled circles: [7]) and HE1327-2326 vs. theoretical SN yields from the two models with different degree of mixing and fallback (see [14]).

The elemental abundance patterns of these HMP stars provide a key to the answer to the above questions. The abundance patterns of HE1327-2326 [11] and HE0107-5240 [7] are quite unusual. The striking similarity of $[Fe/H]$ ($=-5.4$ and -5.2 for HE1327-2326 and HE0107-5240, respectively) and $[C/Fe]$ ($\sim +4$) suggests that similar chemical enrichment mechanisms operated in forming these HMP stars. However, the N/C and $(Na, Mg, Al)/Fe$ ratios are more than a factor of 10 larger in HE1327-2326. In order for the theoretical models to be viable, these similarities and differences should be explained self-consistently.

Iwamoto et al. [14] showed that the above similarities and variations of the HMP stars can be well reproduced in unified manner by nucleosynthesis in the core-collapse “faint” SNe which undergo mixing-and-fallback (Fig.5: right). Iwamoto et al. [14] thus argue that the HMP stars are the second generation low mass stars, whose formation was induced by the Pop III SN with efficient cooling of carbon-enriched gases.

3. Discussion

3.1 GRB Connection

We have shown that a faint SN as a result of large fallback is responsible to produce the carbon enhanced patterns of extremely metal-poor (CEMP) stars. The fallback SN [14, 12] should also undergo mixing of ^{56}Ni before the occurrence of fallback in order to reproduce the observed light curve. Tominaga (2009) has shown that such “mixing and fallback” in spherical explosion is equivalent to the jet-induced nucleosynthesis [27].

In the jet-induced nucleosynthesis and mass ejection, the important parameter is the energy deposition rate \dot{E}_{dep} [25]. The variation of \dot{E}_{dep} in the range of $\dot{E}_{\text{dep},51} \equiv \dot{E}_{\text{dep}}/10^{51} \text{ergs s}^{-1} = 0.3 - 1500$ leads to the following variation of the properties of GRBs and associated SNe. For low energy deposition rates ($\dot{E}_{\text{dep},51} < 3$), the ejected ^{56}Ni masses ($M(^{56}\text{Ni}) < 10^{-3}M_{\odot}$) are smaller than the upper limits for non-SN GRBs 060505 and 060614 [14]. For intermediate energy deposition rates ($3 \lesssim \dot{E}_{\text{dep},51} < 60$), the explosions eject $10^{-3}M_{\odot} \lesssim M(^{56}\text{Ni}) < 0.1M_{\odot}$, and the final BH masses are $10.8M_{\odot} \lesssim M_{\text{BH}} < 15.1M_{\odot}$. The resulting SN is faint ($M(^{56}\text{Ni}) < 0.01M_{\odot}$) or sub-luminous ($0.01M_{\odot} \lesssim M(^{56}\text{Ni}) < 0.1M_{\odot}$).

In the jet-induced explosion model, the abundance patterns of EMP stars (esp. $[C/Fe]$) are related to \dot{E}_{dep} as follows. Lower \dot{E}_{dep} yields larger M_{BH} and thus larger $[C/Fe]$, because the infall reduces the amount of inner core material (Fe) relative to that of outer material (C) [25]. The abundance patterns of the averaged normal EMP stars, the CEMP star CS 22949–37, and the two HMP stars (HE 0107–5240 and HE 1327–2326) are well reproduced by the models with $\dot{E}_{\text{dep},51} = 120, 3.0, 1.5,$ and $0.5,$ respectively. The model for the normal EMP stars ejects $M(^{56}\text{Ni}) \sim 0.2M_{\odot}$, i.e., a factor of 2 less than SN 1998bw. On the other hand, the models for the CEMP and the HMP stars eject $M(^{56}\text{Ni}) \sim 8 \times 10^{-4}M_{\odot}$ and $4 \times 10^{-6}M_{\odot}$, respectively.

To summarize, (1) the explosions with large energy deposition rate, \dot{E}_{dep} , are observed as GRB-HNe, and their yields can explain the abundances of normal EMP stars, and (2) the explosions with small \dot{E}_{dep} are observed as GRBs without bright SNe and can be responsible for the formation of the CEMP and the HMP stars. We thus propose that GRB-HNe and GRBs without bright SNe belong to a continuous series of BH-forming massive stellar deaths with relativistic jets of different \dot{E}_{dep} .

3.2 Concluding Remarks

We report on the properties and nucleosynthesis of the two distinct new classes of massive SNe: 1) very energetic Hypernovae, whose kinetic energy is more than 10 times the KE of normal core-collapse SNe, and 2) very faint and low energy SNe (Faint SNe). These two new classes of SNe are likely to be “black-hole-forming” SNe with rotating or non-rotating black holes. Nucleosynthesis in Hypernovae is characterized by larger abundance ratios (Zn,Co,V,Ti)/Fe than normal SNe, which can explain the observed ratios in EMP stars. Nucleosynthesis in Faint SNe is characterized by a large amount of fall-back, which explains the abundance pattern of the most Fe-poor stars.

These comparisons suggest that black-hole-forming SNe made important contributions to the early Galactic (and cosmic) chemical evolution. We discuss how nucleosynthetic properties resulted from such unusual supernovae are connected with the unusual abundance patterns of extremely metal-poor stars. Such connections may provide important constraints on the properties of first stars.

This research has been supported in part by World Premier International Research Center Initiative, MEXT, and by the Grant-in-Aid for Scientific Research of the JSPS (23540262, 23224004) and MEXT (22012003, 23105705), Japan.

References

- [1] Aoki, W., Norris, J. E., Ryan, S. G., Beers, T. C., Christlieb, N., Tsangarides, S., & Ando, H. 2004, *ApJ* 608, 971
- [2] Beers, T. C. & Christlieb, N. 2005, *ARAA* 43, 531
- [3] Bessell, M. S., & Christlieb, N. 2005, in *IAU Symp 228, From Lithium to Uranium*, ed. V. Hill et al. (Cambridge: Cambridge Univ. Press) 237
- [4] Caffau, E., et al. 2011, *Nature* 477, 67

- [5] Cayrel, R., et al. 2004, *A&A* 416, 1117
- [6] Christlieb, N., et al. 2002, *Nature* 419, 904
- [7] Christlieb, N., Gustafsson, B., Korn, A. J., Barklem, P. S., Beers, T. C., Bessell, M. S., Karlsson, T., & Mizuno-Wiedner, M. 2004, *ApJ* 603, 708
- [8] Cooke, R., Pettini, M., Steidel, C. C., King, L. J., Rudie, G. C., & Rakic, O., 2010a, *MNRAS* 409, 679
- [9] Cooke, R., Pettini, M., Steidel, C. C., Rudie, G. C., & Jorgenson, R. A. 2010b, *MNRAS* 412, 1047
- [10] Depagne, E., et al. 2002, *A&A* 390, 187
- [11] Frebel, A., et al. 2005, *Nature* 434, 871
- [12] Fryer, C., et al. 2009, *ApJ* 707, 193
- [13] Heger, A., & Langer, N. 2000, *ApJ* 544, 1016
- [14] Iwamoto, N., Umeda, H., Tominaga, N., Nomoto, K., & Maeda, K. 2005, *Science* 309, 451
- [15] Kobayashi, C., Umeda, H., Nomoto, K., Tominaga, N., & Ohkubo, T. 2006, *ApJ* 653, 1145
- [16] Kobayashi, C., Tominaga, N., & Nomoto, K. 2011, *ApJ* 730, L14
- [17] Maeder, A. & Meynet, G. 2000, *ARAA* 38, 143
- [18] Nissen, P. E., Primas, F., Asplund, M., & Lambert, D. L., 2002, *A&A* 390, 235
- [19] Nomoto, K., et al. 2003, in *IAU Symp 212, A Massive Star Odyssey, from Main Sequence to Supernova*, eds. V. D. Hucht, et al. (San Francisco: ASP) 395 (astro-ph/0209064)
- [20] Nomoto, K., Tominaga, N., Umeda, H., & Kobayashi, C. 2005, in *IAU Symp 228, From Lithium to Uranium*, ed. V. Hill et al. (Cambridge: Cambridge Univ. Press) 287 (astro-ph/0603433)
- [21] Nomoto, K., et al. 2006, *Nuclear Phys A* 777, 424 (astro-ph/0605725)
- [22] Norris, J. E., Christlieb, N., Korn, A. J., Eriksson, K., Bessell, M. S., Beers, T. C., Wisotzki, L., & Reimers, D. 2007, *ApJ* 670, 774
- [23] Ryan, S. G., Norris, J. E., & Beers, T. C. 1996, *ApJ* 471, 254
- [24] Suda, T., Aikawa, M., Machida, M. N., Fujimoto, M. Y., & Iben, I., Jr. 2004, *ApJ* 611, 476
- [25] Tominaga, N., Maeda, K., Umeda, H., Nomoto, K., Tanaka, et al. 2007a, *ApJ* 657, L77
- [26] Tominaga, N., Umeda, H., & Nomoto, K. 2007b, *ApJ* 660, 516
- [27] Tominaga, N. 2009, *ApJ* 690, 526
- [28] Tominaga, N. et al. 2012, in preparation
- [29] Tumlinson, J. 2006, *ApJ* 641, 1
- [30] Umeda, H., Nomoto, K., & Nakamura, T. 2000, in *The First Stars*, ed. A. Weiss, T. Abel, & V. Hill (Berlin: Springer), 150
- [31] Umeda, H., & Nomoto, K. 2002, *ApJ* 565, 385
- [32] Umeda, H., & Nomoto, K. 2003, *Nature* 422, 871
- [33] Umeda, H. & Nomoto, K. 2005, *ApJ* 619, 427
- [34] Weiss, A., Serenelli, A., Kitsikis, A., Schlattl, H., Christensen-Dalsgaard, J. 2005, *A&A* 441, 1129
- [35] Woosley, S. E. & Bloom, J. S. 2006, *ARAA* 44, 507